



PERGAMON

Pattern Recognition ■■■ (■■■) ■■■-■■■

PATTERN
RECOGNITION

THE JOURNAL OF THE PATTERN RECOGNITION SOCIETY

www.elsevier.com/locate/patcog

A combination model for orientation field of fingerprints

Jinwei Gu^a, Jie Zhou^{a,*}, David Zhang^b^aDepartment of Automation, Tsinghua University, Beijing 100084, China^bBiometrics Technology Centre, Department of Computing, Hong Kong Polytechnic University, Kowloon, Hong Kong

Received 6 December 2002; accepted 14 May 2003

Abstract

Orientation field is a global feature of fingerprints that is very important in automatic fingerprint identification systems (AFIS). Establishing an accurate and concise model for orientation fields will not only improve the performance of orientation estimation, but also make it feasible to apply orientation information in the matching process. In this paper, a novel model for the orientation field of fingerprints is proposed. We use a polynomial model to approximate the orientation field globally and a point-charge model at each singular point to improve the approximation locally. These two models are combined together by a weight function. Experimental results are provided to illustrate the fact that this combination model is more accurate and robust with respect to noise compared with the previous works. The application of the model is discussed at the end.

© 2003 Published by Elsevier Ltd on behalf of Pattern Recognition Society.

Keywords: Fingerprint identification; Orientation field; Polynomial model; Point-charge model; Weighting factor

1. Introduction

Among various biometric techniques, automatic fingerprint identification systems (AFIS) are the most popular and reliable for automatic personal identification. During the last years, fingerprint identification has received increasing attention and the performance of fingerprint identification systems has reached a high level. However, it is still not satisfactory for a large database or fingerprints with poor quality [1,2].

A fingerprint is the pattern of ridges and valleys on the surface of a fingertip. In Fig. 1(a), a fingerprint is depicted. In this figure, the ridges are black and the valleys are white. Its *orientation field*, defined as the local orientation of the ridge-valley structures, is shown in Fig. 1(b). The *minutiae*, ridge endings and bifurcations, and the *singular points*, are also shown in Fig. 1(a). Singular points can be viewed as points where the orientation field is discontinuous. They can be classified into two types: A *core* is the point of the

innermost curving ridges and a *delta* is the center of triangular regions where three different directional flows meet. Most classical AFIS algorithms [1–5] take the minutiae and the singular points, including their coordinates and direction, as the distinctive features to represent the fingerprint in the matching process. But this kind of representation does not utilize all available features in fingerprints and therefore cannot provide enough information for large-scale fingerprint identification tasks [6].

As a global feature, orientation field describes one of the basic structures of a fingerprint. The variation of orientation field is of low frequency so that it is robust with respect to various noises. It has been widely used for minutiae extraction and fingerprint classification, but rarely utilized into the matching process. In this paper, we focus on the modeling of orientation field. Our purpose is to represent the orientation field in a complete and concise form so that it can be accurately reconstructed with several coefficients. This work is significant in three ways: (a) It can be used to improve the estimation of orientation field, especially for poor-quality fingerprints, therefore it will be of benefit in the extraction of minutiae for conventional fingerprint identification algorithms. (b) More importantly, the coefficients

* Corresponding author. Tel.: +86-10-6278-2447; fax: +86-10-6278-6911.

E-mail address: jzhou@tsinghua.edu.cn (J. Zhou).

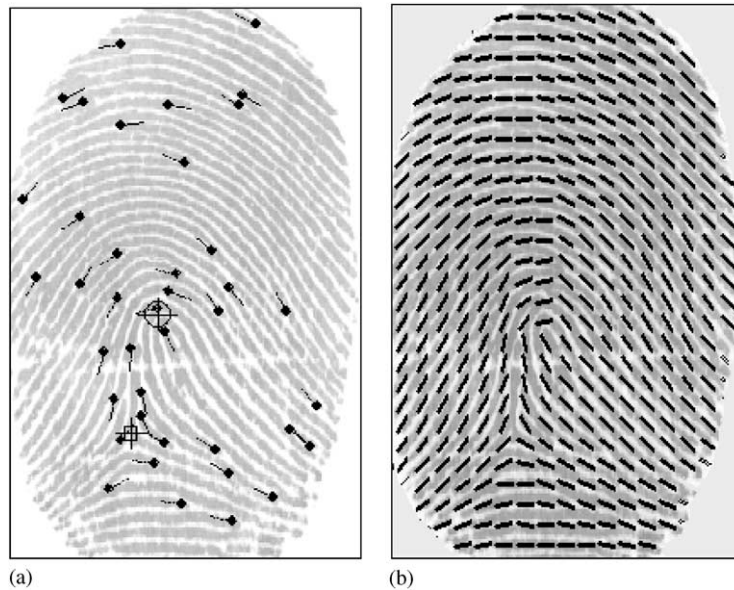


Fig. 1. Example of a fingerprint: (a) singular points and minutiae with its direction; (b) orientation field shown with unit vector.

of the orientation field model can be saved for use in the matching step. As a result, information on orientation field can be utilized for fingerprint identification. By combining it with the minutiae information, a much better identification performance can be expected. (c) In Ref. [7], the authors proposed to synthesize the fingerprint by using information on orientation field, minutiae and the density between the ridges. This makes it possible to establish a complete representation for the fingerprint by combining the orientation model with some other information.

Sherlock and Monro [8] proposed a so-called zero-pole model for orientation field based on singular points, which takes the core as zero and the delta as a pole in the complex plane. The influence of a core, z_c , is $\frac{1}{2} \arg(z - z_c)$ for point z , and that of a delta, z_d , is $-\frac{1}{2} \arg(z - z_d)$. The orientation at z , is the sum of the influence of all cores and deltas. It is simple and effective, but inaccurate because many fingerprints that have the same singular points may yet differ in detail. Vizcaya and Gerhardt [9] have made an improvement using a piecewise linear approximation model around singular points to adjust the zero and pole's behavior. First, the neighborhood of each singular point is uniformly divided into eight regions and the influence of the singular point is assumed to change linearly in each region. An optimization implemented by gradient-descent is then performed to get a piecewise linear function. These two models cannot deal with fingerprint without singular point such as the plain arch classified by Henry [10]. Furthermore, since they do not consider the distance from singular points and the influence of a singular point is the same as any point on the same central line, whether near or far from the singular point, serious

error will be caused in the modeling of the regions far from singular points. As a result, these two models cannot be used for accurate approximation to real fingerprint's orientation field.

Here we propose a combination model for the orientation field. Since the orientation of fingerprints is quite smooth and continuous except at singular points, we apply a polynomial model to approximate the global orientation field. At each singular point, a point-charge model similar to the zero-pole model is used to describe the local region. Then, these two models are combined smoothly together through a weight function. The advantages of our combination model are as below: (1) It can accurately represent the orientation field at regions either near or far from singular points. (2) Global approximation makes it robust against noise. (3) It has a concise representation, which guarantees a low storage cost for its application to fingerprint identification.

The paper is organized as follows. In Section 2, the combination model of the orientation field is proposed. The algorithm for computing the model's coefficients is given in Section 3. Experimental results are presented in Section 4. We finish with conclusions and discussion on applications of our model.

2. The combination model of orientation field

From Fig. 1(b), we can see that the orientation pattern of a fingerprint is quite smooth and continuous except near the singular points. That means we can apply a simple and smooth function to approximate it globally.

1 Since the value of a fingerprints' orientation is defined
 2 within $[0, \pi)$, it seems that this representation has an intrinsic
 3 discontinuity (in fact, the orientation, 0, is the same as the
 4 orientation, π , in ridge pattern). So we cannot model the
 5 orientation field directly. A solution to this problem is to
 6 map the orientation field to a continuous complex function.
 7 Define $\theta(x, y)$ and $U(x, y)$ to be, respectively, the orientation
 8 field and the transformed function, respectively. The
 9 mapping can be defined as

$$U = R + iI = \cos 2\theta + i \sin 2\theta, \quad \theta \in [0, \pi), \quad (1)$$

10 where R and I denote, respectively, the real part and imag-
 11 inary part of the complex function, $U(x, y)$. Obviously,
 12 $R(x, y)$ and $I(x, y)$ are continuous with x, y in those re-
 13 gions. The above mapping is a one-to-one transformation
 14 and $\theta(x, y)$ can be easily reconstructed from the values of
 15 $R(x, y)$ and $I(x, y)$.

16 Now, the modeling of the orientation field can be done in
 17 two ways. One is to model the complex function, $U(x, y)$,
 18 in the complex domain directly; the other is to model its
 19 real part, $R(x, y)$, and imaginary part, $I(x, y)$, respectively,
 20 in the real domain. We employ the second method in this
 21 paper; the former method will be addressed in our future
 22 research.

23 To globally represent $R(x, y)$ and $I(x, y)$, two bivariate
 24 polynomial models are established, which are denoted by
 25 PR and PI , respectively. These two polynomials can be for-
 26 mulated as

$$PR(x, y) = (1 \quad x \quad \cdots \quad x^n) \cdot P_1 \cdot \begin{pmatrix} 1 \\ y \\ \vdots \\ y^n \end{pmatrix} \quad (2)$$

27 and

$$PI(x, y) = (1 \quad x \quad \cdots \quad x^n) \cdot P_2 \cdot \begin{pmatrix} 1 \\ y \\ \vdots \\ y^n \end{pmatrix}, \quad (3)$$

28 where n is the polynomials' order and the matrices,
 29 $P_i \in \mathfrak{R}^{n \times n}$, $\forall i = 1, 2$.

30 Near the singular points, the orientation is no longer
 31 smooth, so it is difficult to model with a polynomial func-
 32 tion. A model named 'point-charge' (PC) is added at each
 33 singular point. And for a certain singular point, its influence
 34 at the point, (x, y) , varies with the distance between the
 35 point and the singular point. Fig. 2(a) shows the unit influ-
 36 ence vector (tangent vector) caused by a standard core. Its
 37 electric flux lines are clockwise along the concentric circle.
 38 The influence of a standard (vertical) core at the point,

(x, y) , is defined as

$$PC_{Core} = H_1 + iH_2 = \begin{cases} \frac{y - y_0}{r} Q + i \frac{x - x_0}{r} Q, & r \leq R, \\ 0, & r > R, \end{cases} \quad (4)$$

39 where (x_0, y_0) is this core's position and $r =$
 40 $\sqrt{(x - x_0)^2 + (y - y_0)^2}$. Because the influence of a core
 41 is just like positive electricity, we call Q as the electrical
 42 quantity. R is defined as the effective radius. The influence
 43 of a standard delta is
 44

$$PC_{Delta} = H_1 + iH_2 = \begin{cases} \frac{y - y_0}{r} Q - i \frac{x - x_0}{r} Q, & r \leq R, \\ 0, & r > R. \end{cases} \quad (5)$$

45 Compared with the model provided in Ref. [8], our
 46 point-charge model uses different quantities of electricity to
 47 describe the neighborhood of each singular point instead of
 48 the same influence at all singular points.
 49

50 In a real fingerprint, the ridge pattern at the singular points
 51 may have a rotation angle compared with the standard one. If
 52 the rotation angle from standard position is ϕ ($\phi \in [-\pi, \pi)$,
 53 see Fig. 2(b)), a transformation can be made as

$$\begin{pmatrix} x' \\ y' \end{pmatrix} = \begin{pmatrix} x_0 \\ y_0 \end{pmatrix} + \begin{pmatrix} \cos \phi & \sin \phi \\ -\sin \phi & \cos \phi \end{pmatrix} \begin{pmatrix} x - x_0 \\ y - y_0 \end{pmatrix}. \quad (6)$$

54 Then, the point-charge model can be modified by taking x'
 55 and y' instead of x and y , for cores in Eq. (4) and deltas in
 56 Eq. (5), respectively.

57 To combine the polynomial model (PR, PI) with
 58 point-charge smoothly, a weight function can be used. For
 59 point-charge, the weighting factor at the point, (x, y) , is
 60 defined as

$$\alpha_{PC}^{(k)}(x, y) = 1 - \frac{r^{(k)}(x, y)}{R^{(k)}}, \quad (7)$$

61 where $(x_0^{(k)}, y_0^{(k)})$ is the coordinate of the k th singular point,
 62 $R^{(k)}$ is the effective radius (as defined in Eqs. (4)–(5)), and
 63 $r^{(k)}(x, y)$ is set as $\min(\sqrt{(x - x_0^{(k)})^2 + (y - y_0^{(k)})^2}, R^{(k)})$.
 64 For the polynomial model, the weighting factor at the point,
 65 (x, y) , is

$$\alpha_{PM}(x, y) = \max \left\{ 1 - \sum_{k=1}^K \alpha_{PC}^{(k)}, 0 \right\}, \quad (8)$$

66 where K is the number of singular points. The weight func-
 67 tion guarantees that for each point, its orientation follows
 68 the polynomial model if it is far from the singular points
 69 and follows the point-charge if it is near one of the singular
 70 points.

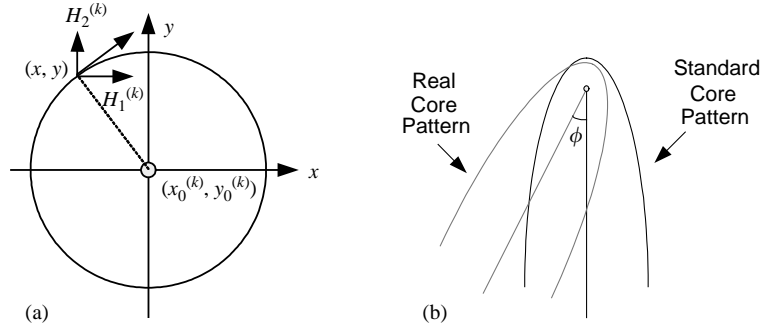


Fig. 2. Point-charge model: (a) influence vector around a standard core; (b) real ridge pattern near a core with a rotation angle, ϕ .

1 Then, the combination model for the whole fingerprint's
2 orientation field can be formulated as

$$\begin{pmatrix} R(x, y) \\ I(x, y) \end{pmatrix} = \alpha_{PM} \cdot \begin{pmatrix} PR \\ PI \end{pmatrix} + \sum_{k=1}^K \alpha_{PC}^{(k)} \cdot \begin{pmatrix} H_1^{(k)} \\ H_2^{(k)} \end{pmatrix}, \quad (9)$$

3 where PR and PI are, respectively, the real and imaginary
4 part of the polynomial model, and $H_1^{(k)}$ and $H_2^{(k)}$ are, respectively,
5 the real and imaginary part of point-charge model for
6 the k th singular point. Obviously, the combination model
7 is continuous with x and y . The coefficient matrices of the
8 two polynomials, PR and PI , and the electrical qualities,
9 $\{Q_1, Q_2, \dots, Q_K\}$, of the singular points will define the combination model.

3. Implement scheme

3.1. Coarse orientation field computation

13 There are essentially two ways to compute the orientation
14 field: filter-bank based approaches [11–13] and
15 gradient-based approaches [4,14–16]. The filter-bank
16 based approaches are more resistant to noise than the
17 gradient-based, but they are discrete-valued (depending on
18 the number of filters) and too computationally expensive.
19 So we adopt a gradient-based approach in our work. The
20 coarse orientation field, O , and its reliability, W , can be
21 obtained, respectively, by

$$O(x, y) = \frac{1}{2} \tan^{-1} \frac{\sum_{\Gamma} 2G_x G_y}{\sum_{\Gamma} (G_x^2 - G_y^2)} + \frac{\pi}{2} \quad (10)$$

and

$$W(x, y) = \frac{(\sum_{\Gamma} (G_x^2 - G_y^2))^2 + 4(\sum_{\Gamma} G_x G_y)^2}{(\sum_{\Gamma} (G_x^2 + G_y^2))^2}, \quad (11)$$

23 where Γ is a small neighboring region of the point, (x, y) ,
24 (G_x, G_y) is the gradient vector at (x, y) , and the output of
25 $\tan^{-1}(\cdot)$ is within $[-\pi, \pi]$.

26 We also need to identify the position and type of singular
27 points. Many approaches have been proposed for singular

point extraction. Most of them are based on the Poincare
index [3,4,16,11]. In this paper, we adopt the algorithm pro-
posed in Ref. [11].

3.2. Polynomial approximation

33 The above two bivariate polynomials can be computed
34 by using the Weighted Least Square (WLS) algorithm [17].
35 The coefficients of the polynomial are obtained by minimizing
36 the weighted square error between the polynomial and
37 the values of $R(x, y)$ and $I(x, y)$ computed from the real
38 fingerprint. As pointed above, the reliability, $W(x, y)$, can
39 indicate how well the orientation fits the real ridge. The higher
40 the reliability $W(x, y)$ is, the more influence the point should
41 have. Then $W(x, y)$ can be used as the weighting factor at
42 the point (x, y) . As a result, it can efficiently decrease the
43 influence of inaccurate orientation estimation.

44 As we know, a higher-order polynomial can provide
45 a better approximation, but at the same time it will result
46 in a much higher cost of storage and computation. Moreover,
47 a high-order polynomial will be ill behaved on numerical
48 approximation. As to a lower-order polynomial, however,
49 it will yield lower approximation accuracy in those regions
50 with high curvature. In our experiments, we have tried 3-order,
51 4-order and 5-order polynomials, respectively, and their
52 performances are listed in Table 1. As a tradeoff, we choose
53 4-order ($n = 4$) polynomials for the global approximation.
54 The experimental results showed that they performed well
55 enough for most real fingerprints, while preserving a small
56 cost for storage and computation.

3.3. Computation of point-charge model

57 The coefficients of the point-charge model at singular
58 points can be obtained in two steps. First, two parameters
59 are estimated for each singular point: the rotation angle, ϕ ,
60 and the effective radius, R . Second, charges of singular points
61 are estimated by optimization.

62 Since the average orientation near the singular point can
63 be inferred from the result of polynomial approximation,

Table 1

The average approximation errors (i.e. the mean error and standard deviation) of the zero-pole model, the piecewise linear model and our combination model with different polynomial order. As a tradeoff, we choose $n = 4$ for the combination model in our study

| | Zero-pole | Piecewise linear | Combination model | | |
|--------------------|-----------|---------------------|----------------------|---------|---------|
| | | | $n = 3$ | $n = 4$ | $n = 5$ |
| Mean | 14.32 | 10.64 | 8.43 | 5.58 | 5.17 |
| Standard deviation | 5.47 | 4.15 | 3.84 | 2.42 | 2.35 |

the rotation angle, ϕ , which can be regarded as the cross angle between the vertical line and the average orientation of the ridge pattern around the singular point, can be easily computed. For cores, we can further tell whether it is upward or downward by matching the core with an upward core and a downward core template, which are generated from the standard point-charge model. For the convenience of computation, we use a same R for each singular point, which can be determined empirically.

After that, we need to estimate the electrical quantity for each singular point. Since our purpose is to minimize the approximation error, the objective function for the singular points can be represented as

$$\min J = \sum_{\Omega} ([R(x, y) - \cos(2O)]^2 + [I(x, y) - \sin(2O)]^2), \quad (12)$$

where O is the original orientation field and Ω is the effective region for the point-charge model. For each singular point, its effective region is a small circle with radius R . Ω is the union of all these small circles. The variables in the above optimization problem are the charges of singular points, $\{Q_1, Q_2, \dots, Q_K\}$. They can be computed by solving the following equations as

$$\partial J / \partial Q_k = 0, \quad k = 1, 2, \dots, K. \quad (13)$$

In Fig. 3, the results of each step in our implement scheme are listed.

4. Experimental results

Experiments are carried on two sets of fingerprints. The first set (Set 1) is a sample database from NIST Special Database 14 [18] that contains 40 fingerprint images. The images' size is 480×512 . The second set (Set 2) contains 60 fingerprint images captured with a live-scanner, whose size is 512×320 . The fingerprints in these two sets vary in quality and type.

Three orientation models are evaluated on the database: the zero-pole model [8], the piecewise linear model [9] and our combination model. All of them use the same algorithm

for singular point extraction and orientation estimation. In global approximation, 4-order bivariate polynomials are employed. As pointed in Ref. [16], there is no ground truth for the orientation field of fingerprints and objective error measurement cannot be constructed. Therefore, it is difficult to evaluate the quality of estimated orientation field quantitatively. Vizcaya and Gerhardt [9] evaluated the approximation error with the original orientation matrix, which is not suitable because the original orientation matrix is often too noisy to meet the real pattern's orientation (see Figs. 5(b) and 6(b) for example). We deal with this problem by two means. First, as mentioned above, the orientation field extracted by a Gabor filter-bank (when the number of filters is large enough) is more reliable than the original one based on gradient computing, we can compute the error of the constructed orientation field by comparing it with the orientation field extracted by using Gabor filter-bank (but it should also be noted that orientation computation based on Gabor filter is too computationally expensive and not suitable for real applications, as mentioned in Section 3.1). Secondly, the quality of the estimation is assessed by means of manual inspection.

In the first one, the approximation error of a fingerprint is defined as the mean absolute error (MAE) on all points between the orientation field reconstructed by the model and the orientation field extracted by the Gabor filter-bank [11] (64-filters), i.e.,

$$MAE = \frac{1}{N} \sum_{(x,y) \in \Omega} d(O_{Recon}(x, y) - O_{Gabor}(x, y)), \quad (14)$$

where Ω is the region of comparison, which contains totally N points, (x, y) is the coordinate of a point in Ω , O_{Recon} and O_{Gabor} denote the reconstructed orientation map and the orientation field computed by Gabor filter bank, respectively. Since the orientation is in $(0, \pi]$, the function $d(\cdot)$ is defined as

$$d(\theta) = \begin{cases} |\theta|, & |\theta| < \frac{\pi}{2}, \\ \pi - |\theta|, & \text{otherwise.} \end{cases} \quad (15)$$

Then, by averaging the total approximation error on all the fingerprints in the database, the error of each model can be obtained along with its standard deviation. The results are summarized in Table 1. The mean error of the approximation is 14.32, 10.64, and 5.58, by using the zero-pole model, the piecewise linear model and our combination model, respectively. The standard deviation is 5.47, 4.75, and 2.42, by using these three models, respectively. The results show that our combination model leads to 47.6% reduction in the mean error and 49.1% reduction in the standard deviation compared with the other two models.

From observation, it can also be concluded that the performance of our combination model is very satisfactory, and much better than the other two models and the Gabor filter-bank based estimation. Some of the results of our combination model are presented in Fig. 4. Among them there are various fingerprint types: loop, whorl, twin loop, and

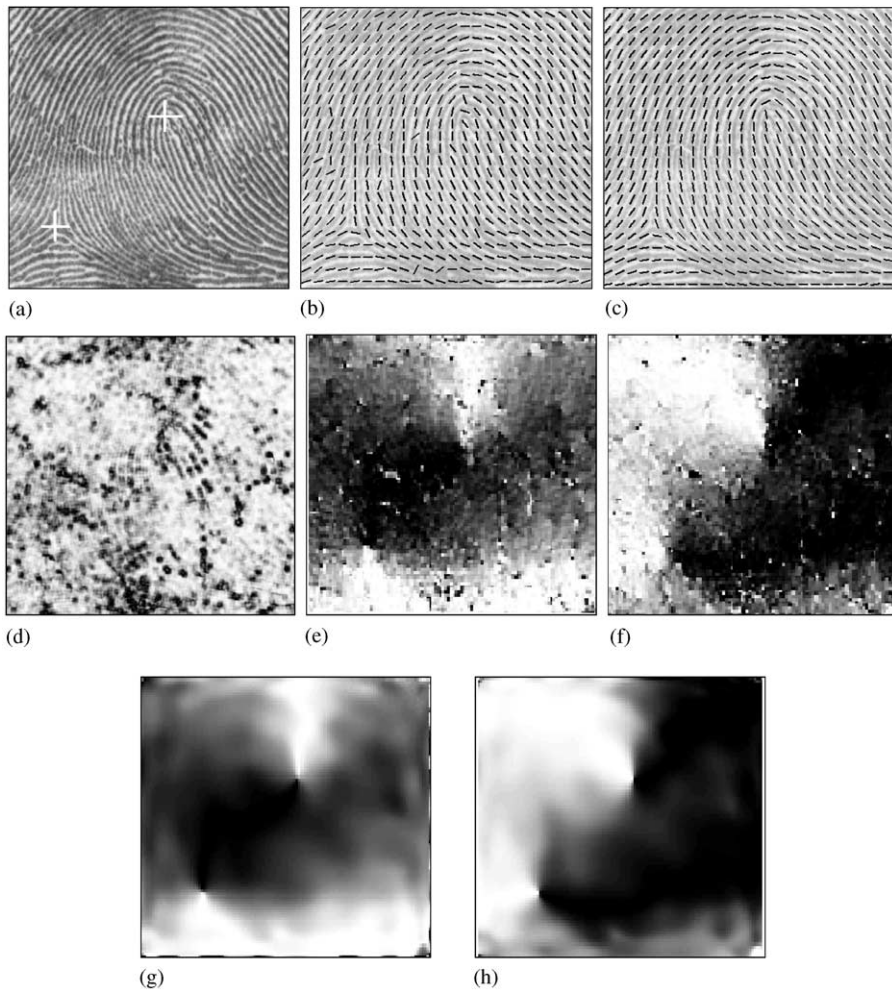


Fig. 3. The results of each step in our implement scheme of the modeling: (a) original fingerprint with singular points marked; (b) the coarse orientation matrix O ; (c) the reconstructed orientation matrix by the combination model; (d) the reliability W ; (e) $\cos(2O)$ and (f) $\sin(2O)$ are the transformed images of the coarse orientation matrix O ; (g, h) transformed images of the reconstructed orientation matrix.

1 plain arch without singular points. It should be noted that the
 2 other two models couldn't deal with plain arch fingerprints.
 3 The reconstructed orientation fields are shown as unit vectors
 4 upon the original fingerprint. We can see that the result is
 5 rather accurate and robust to noise.

6 Figs. 5 and 6 give two examples for comparison. (a)
 7 is the input fingerprint; (b) is the original orientation field
 8 for approximation obtained by gradient-based method [14];
 9 (c) is the orientation field by Gabor filter-bank (64 filters)
 10 method [16]; while (d–f) are the orientation fields recon-
 11 structed, respectively, by the zero-pole model, the piecewise
 12 linear model and our own combination model. From the re-
 13 sults, we can see that: (1) For poor-quality fingerprints, the
 14 gradient-based method (see Figs. 5(b) and 6(b)) can only
 15 extract the orientation field coarsely with much noise. The
 16 Gabor filter-bank based method (see Figs. 5(c) and 6(c)) is

17 better, however, it is still heavily influenced by noise such
 18 as creases and scars. The combination model, though based
 19 on the coarse orientation field, can reconstruct the orienta-
 20 tion field smoothly and accurately against the noise. Thus it
 21 can be used to improve the orientation field estimation. (2)
 22 Among these three models, the zero-pole model can only
 23 roughly describe the orientation (see Figs. 5(d) and 6(d)).
 24 The piecewise linear model does better near the singular
 25 points, but it fails in places far from them, as can easily be
 26 observed at the right bottom part in Fig. 5(e) and the top part
 27 and bottom part in Fig. 6(e). By contrast, the combination
 28 model can describe the orientation of the whole fingerprint
 29 image smoothly and precisely, whether the region is near or
 30 far from the singular points.

31 In our experiments, the combination model has a sat-
 32 isfying performance for most fingerprint images. But the

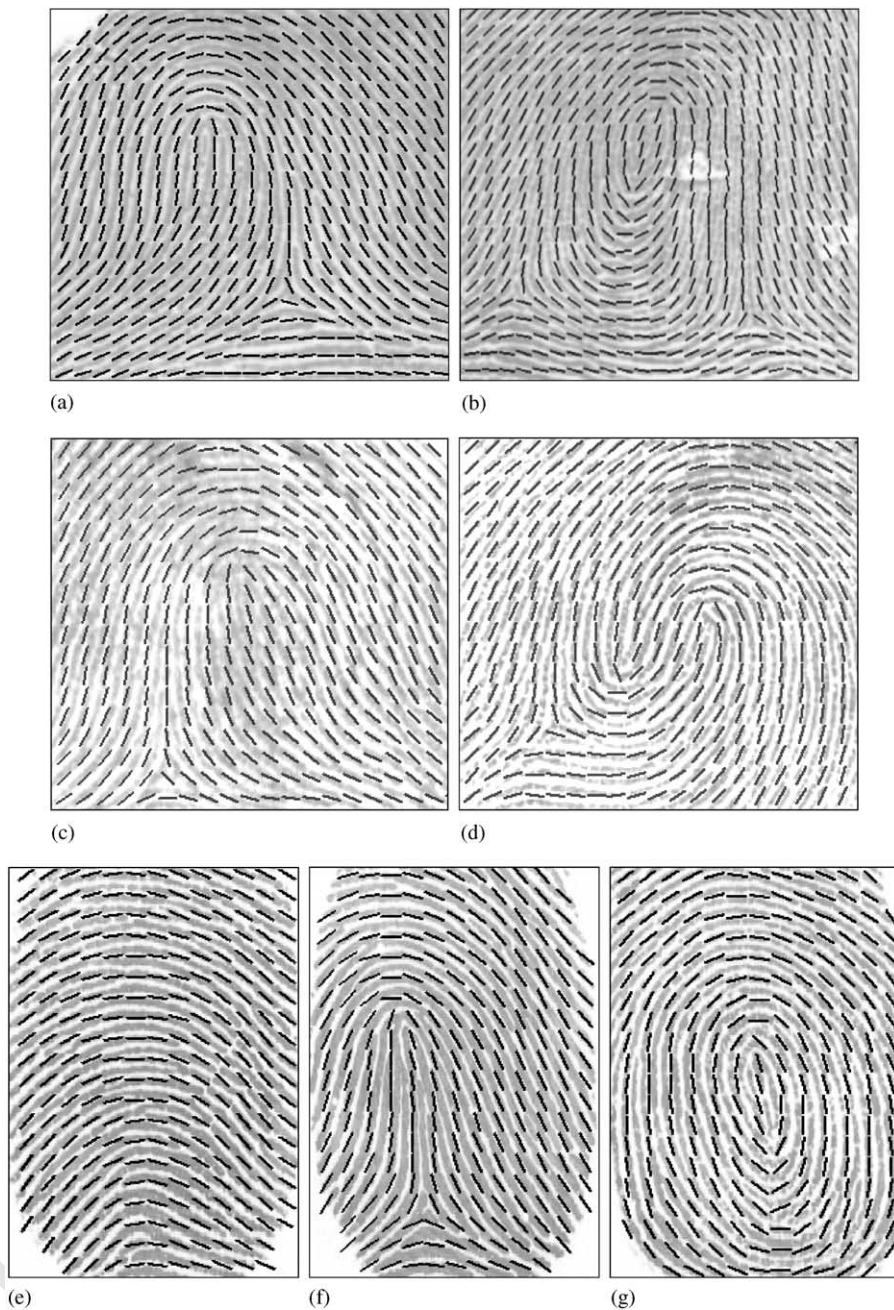


Fig. 4. Examples of reconstructed orientation field by the combination model: (a–d) from Set 1; (e–g) from Set 2. Various types of fingerprint are among them. (e) is a plain arch without singular point modeled only with polynomial model. In contrast, zero-pole and piecewise linear model cannot deal with the plain arch as (e).

1 model's parameters are computed by an approximation
 2 procedure, so they are heavily influenced by the results
 3 of original orientation field estimation and singular points
 4 extraction. For a few poor-quality fingerprints, if the original
 5 orientation field is too unreliable, or if one cannot

extract the singular points correctly at all, the approximation
 performance of the combination model will be bad. In Fig. 7, an example is given, in which (a) is the
 input fingerprint; (b) is the original orientation field for
 approximation obtained by gradient-based method; and

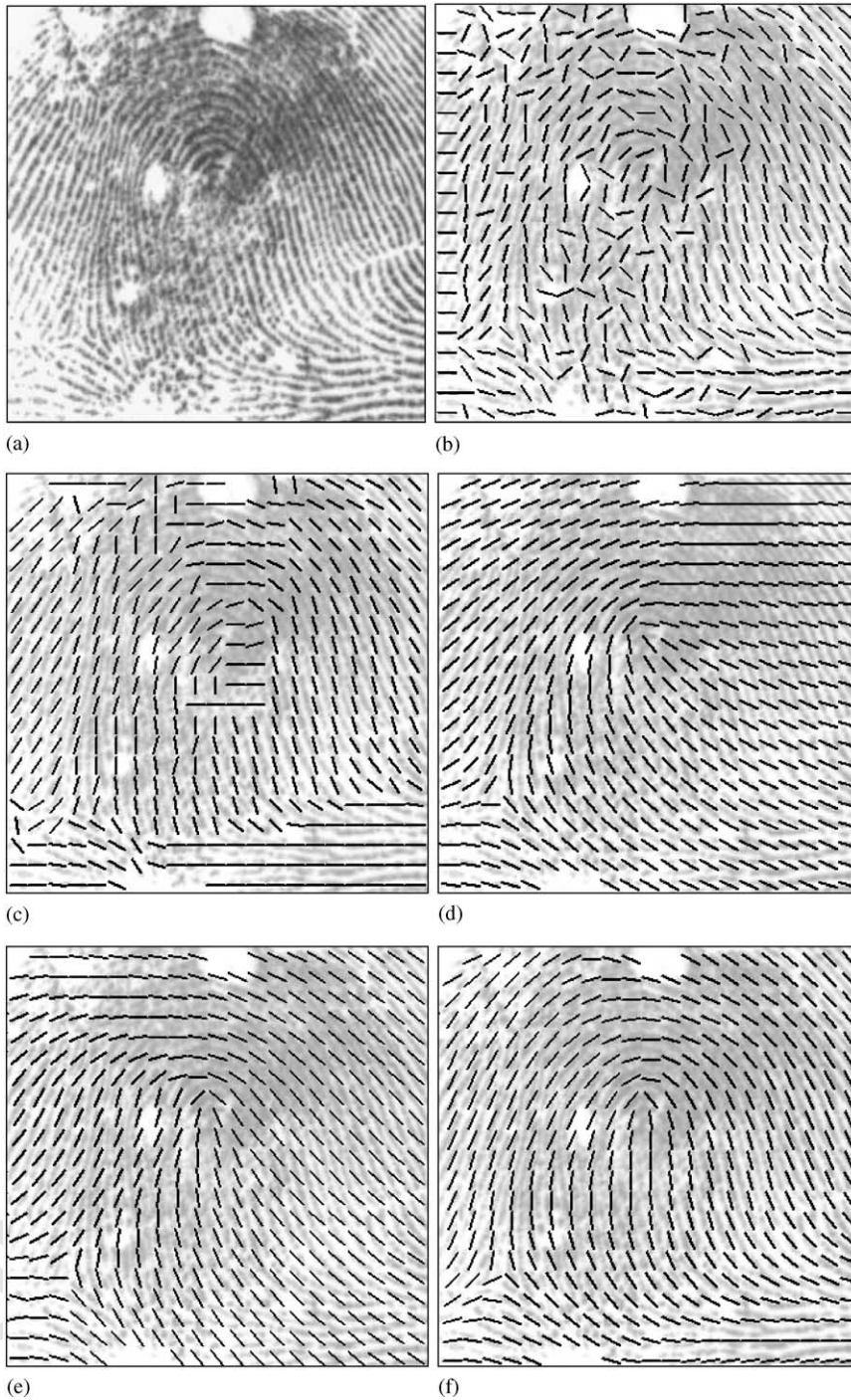


Fig. 5. Comparative result I: (a) original fingerprint; (b) estimated by gradient-based method [14]; (c) estimated by Gabor filter-bank (64 filters) method [16]; (d) reconstructed by zero-pole model; (e) reconstructed by piecewise linear model; (f) reconstructed by the combination model.

1 (c) is the orientation fields reconstructed by our combi-
 2 nation model. Since (a) is too noisy in the right-bottom
 3 part, there is no reliable orientation information in (b).

Consequently, the orientation field reconstructed by our
 combination model will fail in the right-bottom part, as
 in (c).

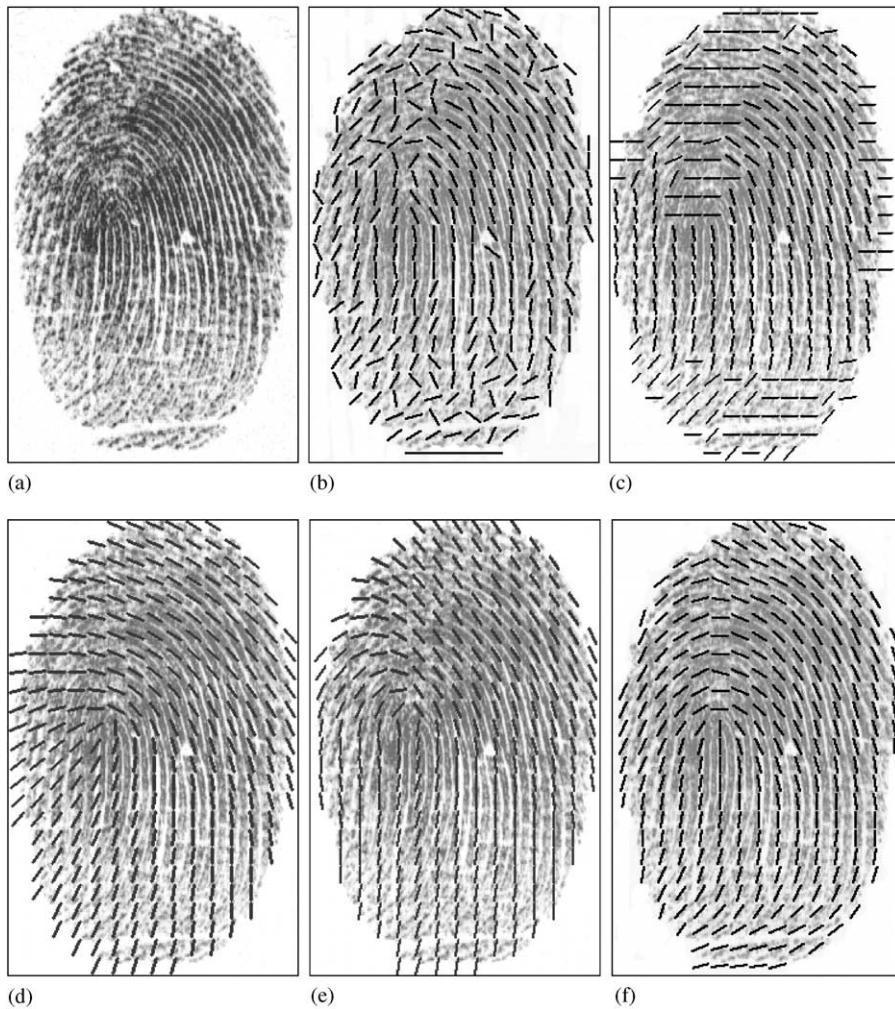


Fig. 6. Comparative result II: (a) original fingerprint; (b) estimated by gradient-based method [14]; (c) estimated by Gabor filter-bank (64 filters) method [16]; (d) reconstructed by zero-pole model; (e) reconstructed by piecewise linear model; (f) reconstructed by the combination model.

1 Most fingerprints have up to 4 singular points (2 cores and
 2 deltas). Assuming that an n -order polynomial is applied
 3 for a fingerprint with 4 singular points, the total number of
 4 coefficients is $2(n+1)^2 + 4$ (2 coefficient matrices for PR and
 5 PI , and 4 charges for modeling singular points). Since n is
 6 chosen as 4 in our study, that means that only 54 coefficients
 7 need to be saved for further usage. As to the computation
 8 cost, about 1 s is required to compute all the coefficients
 9 when the entire process is implemented with Matlab 6.1 and
 C on a Pentium III 500 Hz PC.

5. Discussions and conclusions

13 In this paper, a combination model for the orientation
 field of fingerprints is proposed, which can approximate the

orientation field accurately and reliably. The experimental
 results show that our model leads to nearly 50% reduction
 in the mean error and standard deviation compared with
 the previous works. Moreover, it can deal with fingerprints
 without singular points and be implemented efficiently for
 on-line processing.

Our future work will go in two directions. First, our combination model deals with the smoothly continuous ridge pattern and singular points separately, and then combines them together. As we mentioned above, directly modeling U in complex domain is an alternative method. A rational function in complex domain may be employed for U , which will be more universal and concise.

Another direction for further work is the application of this model. First, as indicated above, minutiae points, orientation map and ridge density map can completely describe

15

17

19

21

23

25

27

29

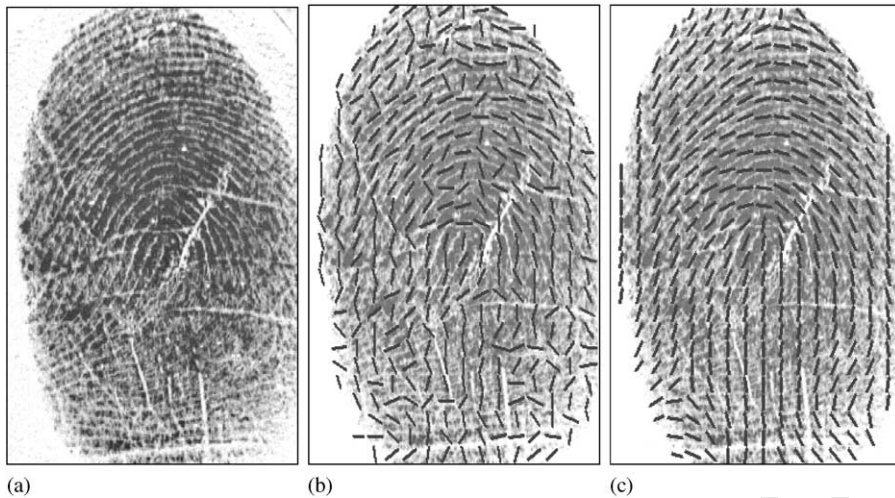


Fig. 7. A failure example of the combination model: (a) input fingerprint; (b) original orientation field for approximation obtained by gradient-based method; (c) orientation fields reconstructed by the combination model. In (a), the original image is too noisy in the right-bottom part and there is no reliable orientation information in that part of (b). Consequently, the orientation field reconstructed by our combination model will fail in that region.

1 a fingerprint image. We can use the orientation model with
 2 other information to compress, restore or synthesize the fin-
 3 gerprint images. Then the noise on the fingerprint images
 4 can be completely removed. Secondly, since the coefficients
 5 of orientation model can be saved and used for fingerprint
 6 matching, we can develop some new methods for fingerprint
 7 identification based on the orientation information and some
 8 other information. As a result, the recognition rate can be
 9 improved.

6. Summary

11 Among various biometric techniques, automatic finger-
 12 print identification is most popular and reliable for automatic
 13 personal identification. Conventional fingerprint identifica-
 14 tion algorithms take the minutiae and the singular points as
 15 the distinctive features to represent the fingerprint. But this
 16 kind of representation cannot provide enough information for
 17 large-scale fingerprint identification tasks.

18 As a global feature, orientation field describes one of the
 19 basic structures of a fingerprint. It has been widely used for
 20 minutiae extraction and fingerprint classification, but rarely
 21 utilized into the matching process. Our purpose is to rep-
 22 resent the orientation field in a complete and concise form.
 23 Its significance lies in: (a) It can be used to improve the es-
 24 timation of orientation field, therefore it will benefit in the
 25 extraction of minutiae for conventional fingerprint identifica-
 26 tion algorithms. (b) More importantly, the coefficients of
 27 the orientation field model can be saved for the use in the
 28 matching stage. As a result, much more information can be
 29 utilized for fingerprint identification. (c) This makes it pos-

sible to establish a complete representation for the finger-
 print by combining the orientation model with some other
 information.

A so-called zero-pole model was proposed for orientation
 field based on singular points, which takes the core as zero
 and the delta as a pole in the complex plane. An improve-
 ment was made by using a piecewise linear approximation
 model around singular points to adjust the zero and pole's
 behavior. Unfortunately, these two models cannot deal with
 fingerprint without singular point such as the plain arch.
 Furthermore, since they consider that the influence of a sin-
 gular point is the same as any point on the same central line
 whether near or far from the singular point, serious error will
 be caused in the modeling of the regions far from singular
 points. As a result, these two models cannot be used for ac-
 curate approximation to real fingerprint's orientation field.

In this paper, we propose a combination model for the
 orientation field. Since the orientation of fingerprints is quite
 smooth and continuous except at singular points, we apply
 a polynomial model to approximate the global orientation
 field globally. At each singular point, a point-charge model
 is used to describe the local region. Then, these two models
 are combined smoothly together through a weight function.
 Experimental results are provided to illustrate the fact that
 this combination model is more accurate and robust with
 respect to noise compared with the previous works. The ad-
 vantages of our combination model are as below: (1) It can
 accurately represent the orientation field at regions either
 near or far from singular points. (2) Global approximation
 makes it robust against noise. (3) It has a concise represen-
 tation, which guarantees a low storage cost for its applica-
 tion to fingerprint identification.

Acknowledgements

The authors wish to acknowledge support from Natural Science Foundation of China under grant 60205002.

References

- 3 [1] A.K. Jain, R. Bolle, S. Pankanti (Eds.), *BIOMETRICS: Personal Identification in Networked Society*, Kluwer Academic Publisher, New York, 1999.
- 5 [2] D. Zhang, *Automated Biometrics: Technologies and Systems*, Kluwer Academic Publisher, USA, 2000.
- 7 [3] K. Hrechak, J.A. McHugh, Automated fingerprint recognition using structural matching, *Pattern Recognition* 23 (1990) 893–904.
- 9 [4] A. Jain, L. Hong, On-line fingerprint verification, *IEEE Trans. Pattern Anal. Mach. Intell.* 19 (4) (1997) 302–314.
- 11 [5] R.S. Germain, A. Califano, S. Colville, Fingerprint matching using transformation parameter clustering, *IEEE Comput. Sci. Eng.* 4 (4) (1997) 42–49.
- 13 [6] S. Pankanti, S. Prabhakar, A.K. Jain, On the individuality of fingerprints, *IEEE Trans. Pattern Anal. Mach. Intell.* 24 (8) (2002) 1010–1025.
- 15 [7] R. Cappelli, A. Erol, D. Maio, D. Maltoni, Synthetic fingerprint-image generation, in: *Proceedings 15th International Conference on Pattern Recognition (ICPR2000)*, Vol. 3, September 2000, pp. 475–478.
- 17 [8] B. Sherlock, D. Monro, A model for interpreting fingerprint topology, *Pattern Recognition* 26 (7) (1993) 1047–1055.
- 19 [9] P. Vizcaya, L. Gerhardt, A nonlinear orientation model for global description of fingerprints, *Pattern Recognition* 29 (7) (1996) 1221–1231.
- 21 [10] E.R. Henry, *Classification and Uses of Finger Prints*, Routledge, London, 1900.
- [11] A. Jain, S. Prabhakar, L. Hong, A multichannel approach to fingerprint classification, *IEEE Trans. Pattern Anal. Mach. Intell.* 21 (4) (1999) 348–359.
- [12] K. Karu, A.K. Jain, Fingerprint classification, *Pattern Recognition* 17 (3) (1996) 389–404.
- [13] A.K. Jain, S. Prabhakar, L. Hong, et al., Filterbank-based fingerprint matching, *IEEE Trans. Image Process.* 9 (5) (2000) 846–859.
- [14] M. Kass, A. Witkin, Analyzing orientated pattern, *Computer Vision, Graphics Image Process.* 37 (1987) 362–397.
- [15] J. Zhou, X. Lu, D. Zhang, C.Y. Wu, Orientation analysis for rotated human face detection, *Image Vision Comput.* 20 (2002) 257–264.
- [16] A.M. Bazen, S.H. Gerez, Systematic methods for the computation of the directional fields and singular points of fingerprints, *IEEE Trans. Pattern Anal. Mach. Intell.* 24 (7) (2002) 905–919.
- [17] P. Whittle, *Prediction and Regulation by Linear Least-Square Methods*, The English Universities Press Ltd., London, 1963.
- [18] NIST Special Database 14: NIST Mated Fingerprint Card Pairs (MFPC2), available at <http://www.nist.gov/srd/nistsd14.htm>.

About the Author—JINWEI GU was born in August 1980. He received B.S. degree from Department of Automation, Tsinghua University, Beijing, China, in 2002. Now he is a master student in Department of Automation, Tsinghua University. His research interests are in pattern recognition and intelligent information processing.

About the Author—DR. JIE ZHOU was born in November 1968. He received B.S. degree and M.S. degree both from Department of Mathematics, Nankai University, Tianjin, China, in 1990 and 1992, respectively. He received Ph.D. degree from Institute of Pattern Recognition and Artificial Intelligence, Huazhong University of Science & Technology (HUST), Wuhan, China, in 1995. From then to 1997, he served as a postdoctoral fellow in Department of Automation, Tsinghua University, Beijing, China. Now he is Associate Professor in Department of Automation, Tsinghua University.

His research area includes Pattern Recognition, Information Fusion, Image Processing and Computer Vision. He has directed or participated more than 10 important projects. In recent years, he has published more than 10 papers in international journals and more than 30 papers in international conferences. He received Best Doctoral Thesis Award from HUST in 1995. Dr. Zhou is a member of IEEE and a fellow of Chinese Association of Artificial Intelligence (CAAI).

About the Author—DAVID ZHANG graduated in computer science from Peking University in 1974 and received the M.Sc. and Ph.D. degrees in computer science and engineering from Harbin Institute of Technology in 1983 and 1985, respectively. From 1986 to 1988, he was a postdoctoral fellow at Tsinghua University and became an associate professor at Academia Sinica, Beijing, China. He received his second Ph.D. in electrical and computer engineering at University of Waterloo, Ontario, Canada, in 1994. Currently, he is a professor in Hong Kong Polytechnic University, Hong Kong. He is Founder and Director of Biometrics Technology Centre supported by UGC/CRC, Hong Kong Government. He also is Founder and Editor-in-Chief, *International Journal of Image and Graphics*, and an associate editor, *Pattern Recognition*, and other five international journals. His research interests include automated biometrics-based identification, neural systems and applications, and parallel computing for image processing & pattern recognition. So far, he has published over 170 papers including seven books around his research areas. Prof. Zhang is a senior member of IEEE.